MultiScience - XXX. microCAD International Multidisciplinary Scientific Conference
University of Miskolc, Hungary, 21-22 April 2016, ISBN 978-963-358-113-1

TIME DEPENDANCE OF WETTING BEHAVIOUR AFTER APPLYING LOW SPATIAL FREQUENCY LIPSS WITH THREE DIFFERENT WAVELENGTHS ON BRASS

Daniel Krysciak[1], Stefan Rung[2], Ralf Hellmann[3]
B.Eng., Master student[1], M.Eng., PhD Student[2]
Prof. Dr., Head of applied laser and photonics group[3]
Applied Laser Technology and Photonics, Hochschule Aschaffenburg, Germany[123]

ABSTRACT

We present investigations on laser induced periodic surface structures on brass to influence the wetting behavior of surfaces. Using ultra short laser pulses with wavelengths of 1030 nm, 515 nm and 343 nm, respectively, large scaled areas completely covered by highly uniformed LIPSS are generated. Beside the applied laser wavelength, the influences of the incident laser fluence and the scribing speed on the contact angle for coverage of the surface with distilled water are examined. To consider time based effects of chemical processes on the solid surface, as being triggered by the laser nano-structuring, the static contact angle was determined daily over two weeks. We observe that firstly the contact angle of all structured samples drops below the contact angle of the polished reference sample. Secondly, we find an increase of the contact angle with time to values in the hydrophobic range. Surfaces structures with LIPSS using 1030 nm showed the highest effect over the investigated time period with an initial contact angle after LIPSS generation of 24° below the reference and a subsequent increase over two weeks to 106°, which in turn is 30° over the reference measurement.

INTRODUCTION

Over the last decade, the increased commercial availability of industrial grade ultra-short pulsed laser systems fostered the application possibilities of this innovative laser source. Beside the advantage of non-thermal material processing, new approaches of structuring methods are intensely investigated. One of these novel applications is the generation of laser induced periodic surface structures (LIPSS), which was firstly observed 1965 by Birnbaum [1]. Generally, LIPSS are separated in two common types. Low spatial frequency LIPSS (LSFL) appear with a spatial periodicity near the incidence laser wavelength whereas high spatial frequency LIPSS (HSFL) show a spatial periodicity clearly below the laser wavelength [2]. The highly increased research in this field reveals the capability to generate LIPSS on metals [3,4], semiconductors [5,6] and dielectrics [7,8]. The generated nanostructures on the surface can lead to benefits in their interaction with their environment and can be used in fields of cell growth [9], friction and wear optimization [10] or emission property of THz transmitter [11]. The influence of LSFL on the wetting properties of surfaces leads to interesting applications like microfluidics [12] and self-cleaning components [13]. The ability of tuning the

DOI: 10.26649/musci.2016.017

wetting properties of laser-treated solids surfaces provides manifold potential applications within afore mentioned areas.

There are fundamentally three different states of wetting behavior differentiated with respect to the contact angle Θ, namely hydrophilic (Θ < 90°), hydrophobic (Θ > 90°) and super-hydrophobic (Θ > 150°). These states can practically be realized either by an additional deposited function layer or by structuring the surface to modify the surface roughness in a specific way. Since the generation of LIPSS depends sensitively on the number of pulses per spot and the used pulse energy, a comprehensive study of feasible laser parameters generally reveals process windows to achieve both, strong hydrophilic states for microfluidics and super hydrophobic states for self-cleaning properties. To deduce the behavior of the contact angle regarding to the generated nanostructures, the interaction process at the solid-liquid interface has to be examined.

WETTABILITY OF LIQUIDS ON SOLIDS

It is commonly accepted that prerequisites for hydrophilic or hydrophobic surfaces are on the one hand the interaction between the interfacial tensions σ of all involved materials and on the other hand the geometric properties of the surface. The first contribution can be described according to the model of Young [14]

$$\boldsymbol{cos\theta_Y = \frac{\sigma_s - \sigma_{sl}}{\sigma_l}} \tag{1}$$

The contact angle θ_Y of a liquid on an ideally flat surface depends solely on the different surface tensions. With σ_s for the surface tension of the solid, σ_{sl} for the interfacial tension between two different or same phases and σ_l for the concluded surface tensions of diffuse and polar proportions.

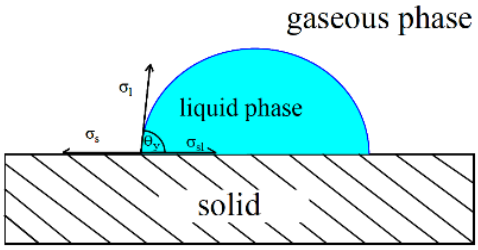

Fig. 1
Contact angle resulting from the Young expression for nominally flat solids

Beside the description by Young, the surface roughness has to be taken into account. Two generally accepted models describe the influence of the geometric properties on the contact angle of liquids on a solid surface. Firstly, the Young model can be advanced to the model of Wenzel [15]. The characterization of Wenzel state is given by complete wetting of a rough solid by any liquid (see fig. 2a). The roughness leads to an increased surface and thus the resulting contact angle decreases below the Young angle. The inherent wetting behavior and the resulting Wenzel contact angle θ_W can be described by:

$$cos\theta_W = \frac{A_T}{A_P} \cdot \frac{\sigma_s - \sigma_{sl}}{\sigma_l} \quad (2)$$

with A_T being the total area which is wetted by a liquid and A_P being the projected area. These two parameters indicate the roughness factor for the contact-angle.

On the other hand, for contact angles above the Young angle the Cassie-Baxter state is used to describe the contact angle, an area in which the Wenzel model fails. The Cassie-Baxter state is characterized by the topography of the surface, which does not allow liquids to get into the valley of surface asperities. Furthermore, the air is trapped into these asperities and remains stable [16]. The difference of Wenzel and Cassie-Baxter states are illustrated in figure 2b. Within the Cassie-Baxter model, a droplet will rests on a composite of chemical surface interface and air. The Cassie-Baxter contact angle θ_{CB} in this case can be described by:

$$cos\theta_{CB} = r' \cdot f_{sl} \cdot \frac{\sigma_s - \sigma_{sl}}{\sigma_l} - 1 + f_{sl} \quad (3)$$

In which f_{sl} is the ratio of the solid/liquid interface in the entire composite surface beneath the liquid and r´ is the roughness of the wetted area. It is worth to stress, that the roughness generated by the laser structures may leads to both, the Wenzel and the Cassie Baxter state, depending on the depth and width of the LSFLs.

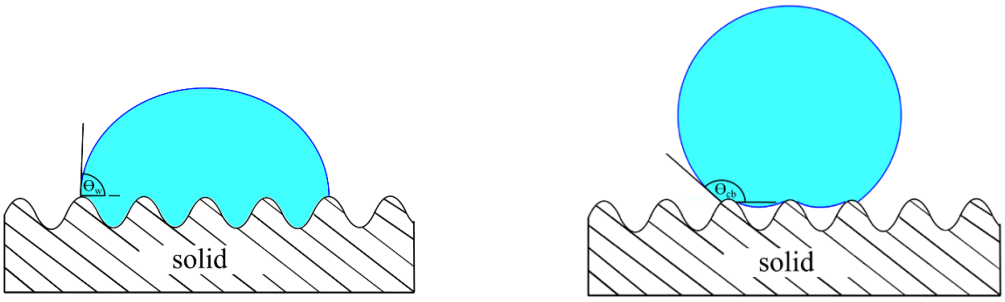

(a) (b)

Fig. 2
Wetting behavior of liquids on rough surfaces regarding to the (a) Wenzel model and the (b) Cassie Baxter model

EXPERIMENTAL

We employed an ultrashort pulsed laser (Pharos 10-600-PP, Light Conversion) with an adjustable pulse duration which, however, is fixed to 220 fs (FWHM) at a repetition rate of 50 kHz in these experiments. Using harmonics generation, we studied the effect of the laser wavelength (1030 nm, 515 nm and 343 nm) on the LIPSS generation and thereby on the wetting behavior. Figure 3a shows the experimental setup for the surface treatment. The energy of the laser beam is adjusted by an external attenuator. With a half wave plate in front of the focusing

unit, the linear polarization of the laser beam is rotated parallel to the onwards used scanning direction. A galvo head (RTA AR800 2G+, Newson) is used in combination with a telecentric lense (f = 100 mm) to focus the beam on the sample.

LSFL are generated on commercial available flat brass (CuZn30) which is cut in square pieces with a size of 16 x 16 mm with a thickness of 0.75mm. The pieces are grinded and polished with a multidirectional polishing machine (LS3V, REMET) with several abrasive strength and afterwards polished with suspensions down to a grain size of 1µm to achieve a reference surface with a roughness Ra between 3 nm to 8 nm. For the examined wetting test, 9 fields with a size of 4.5 x 4.5 mm² are generated by laser irradiation on the brass sample. Each field represents an individual parameter set consisting of altering laser fluence and pulse overlap (i.e. scribing speed). Figure 3b illustrates the sample layout for the experiments using a laser wavelength of 1030 nm. Every parameter set results in a specific line width, hence the line spacing is adapted in each field to achieve similar LSFL generation.

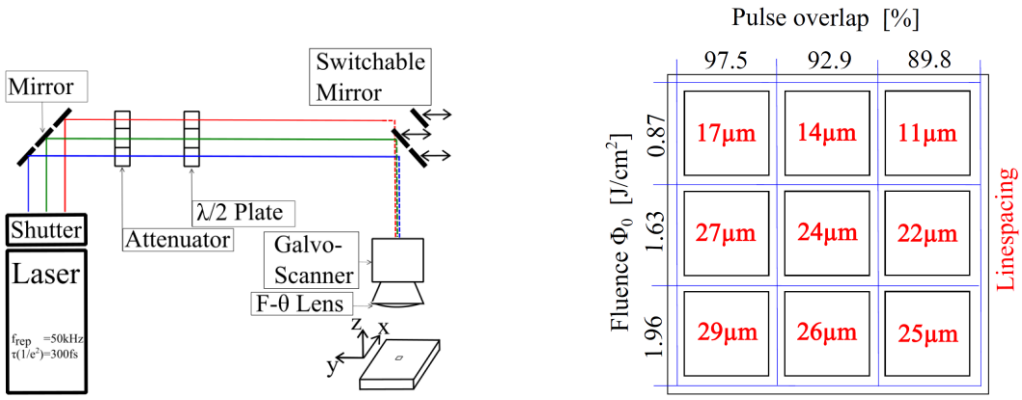

(a) (b)

Fig. 3
Schematic laser setup with three different wavelengths (a) to produce test structures on brass with different parameter sets (b)

The wetting behavior is investigated using a contact angle measurement system (OCA 25, Data Physics) working with the shown schematic method depicted in Fig. 4a. Using a dispensing unit, a droplet (7µL) of distilled water with a surface tension of 74,3 mN/m is deposited on the examined surface. A camera captures the droplet on the surface, the image of which is analyzed by the system software to determine the resulting contact angle (see fig 4b).

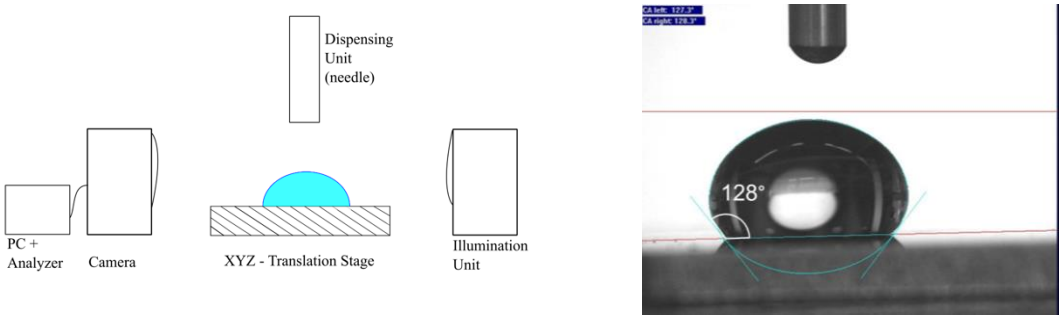

(a) (b)

Fig. 4
(a) Schematic built up of the OCA 25 and (b) process of one static contact angle measurement

Studies by Kietzig et al. [17] and Martínez-Calderon et al. [18] have shown, that the contact angle of water on laser structured surfaces depends on the time between the structuring process itself and the actual measurement. To evaluate this effect specifically on laser induced periodic surface structures, for each laser wavelength ten identical samples were produced at the start of the experiment, allowing measurements of the contact angle on previously unused specimen during ten successive days. All samples were stored under ambient air and a temperature of approximately 23 °C until they were measured.

RESULTS

In a first step, a parameter study for the generation of LSFL on brass is performed with the laser wavelengths 1030 nm, 515 nm and 343 nm (with pulse duration of 220 fs at a repetition of 50 kHz). By altering the laser fluence and the pulse overlap, a two dimensional parameter array is generated to identify the regimes in which LSFLs appear. Based on this preliminary parameter study, for each wavelength nine possible combinations arose using three different values for laser fluence and pulse overlap. The width of the generated lines is measured and used as line pitch to generate the 4.5 x 4.5 mm² fields. Figure 5 exemplarily depicts a structured surface using a laser wavelength of 1030 nm, a fluence of 0.87 J/cm², a scribing overlap of 97.5 % and a line pitch of 17 µm. The LSFL appear orthogonal to the laser polarization and apparently the LSFL are connected to each other, thus covering the brass homogenously.

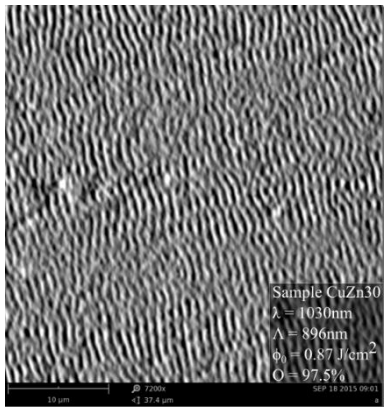

Fig. 5
LSFL on brass using 1030nm fs laser beam, scribing direction from left to right.

Figure 6 summarizes the time dependence of the contact angle over ten days for each wavelength (error bars represent the spread of all nine parameter sets). For comparative reasons, also the reference contact angle is shown in these diagrams. On the first day of the study, the contact angle was measured directly after laser structuring. Apparently, the contact angle for surfaces structured with 1030 nm and

515 nm drops below the polished reference to a hydrophilic state (cf. Fig. 6a and 6b). During the next two days the contact angle rises sharply, while this increase slows down during the following days. Moreover, while the contact angle for LIPSS generated with 515nm remains almost constant at a level of 93° after six days, it continues to grow up to 106° for LIPSS created by a laser wavelength of 1030nm.

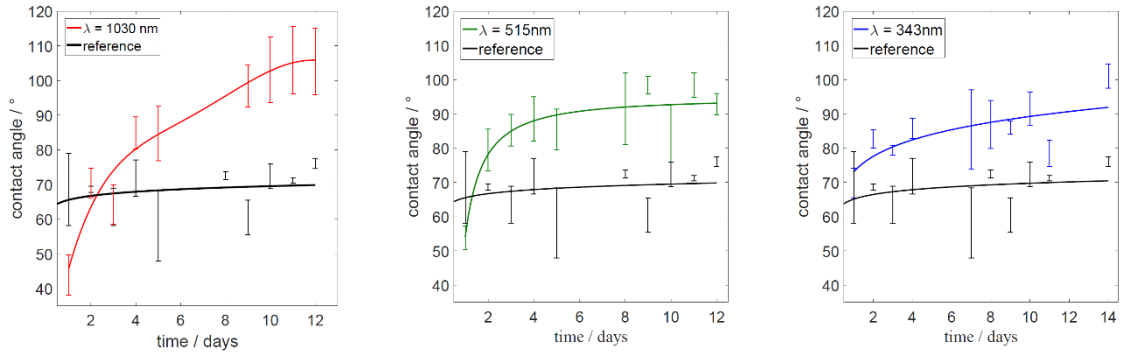

(a) (b) (c)

Fig. 6
Contact angle after laser irradiation with (a) 1030nm, (b) 515nm and (c) 343nm. The solid lines represent the trend line.

Contrary to this observation, the contact angle on LIPSS generated using a UV wavelength of 343nm is higher as compared to the polished reference sample and rises further during the next days up to 92° (Fig. 6c). According to Ref. 17 and 18, the contact angle shows his major time dependence during the first two weeks after structuring the surface. Own spot measurements during a period of over four weeks, however, reveal no appreciable further change of the contact angle on this time scale. Though this temporal behavior of the contact angle is still under controversial discussion within the scientific community, the chemical interaction with ambient carbon dioxide is identified to play a crucial role, leading to an accumulation of carbon compounds on the irradiated surface [17].

It is worthwhile to note, that LIPSS generated with a laser wavelength of 1030nm reveal not only the highest drop of the contact angle directly after irradiation but also exhibit the highest resulting contact angles after several days.

Figure 7 shows the fitting functions (power fitting, $a * x^b + c$) of the measured contact angles for the experiments using 1030 nm. Fig. 7a compares the temporal evolution of the contact angle for different laser fluences and Fig. 7b summarizes the influence of pulse overlap, respectively. In both cases, the parameter with the highest initial drop after irradiation finally leads to the highest value of the contact angle after 12 days, i,e. LIPSS generated with high laser fluence and a high pulse overlap are preferential for a high contact angle increase. High laser fluence and high pulse overlap result in a high energy deposition into the irradiated material and preliminary experiments reveal, that a higher energy deposition leads to a smaller periodicity of the LSFL structures. In this study, the periodicity of LSFL is in the range of 740 nm for higher energy deposition and about 940 nm for lower energy deposition. With respect to the Cassie-Baxter model, we attribute this experimental

observation to the different geometries (periodicity and modulation depth) of the LIPSS generated with different wavelengths and energy depositions.

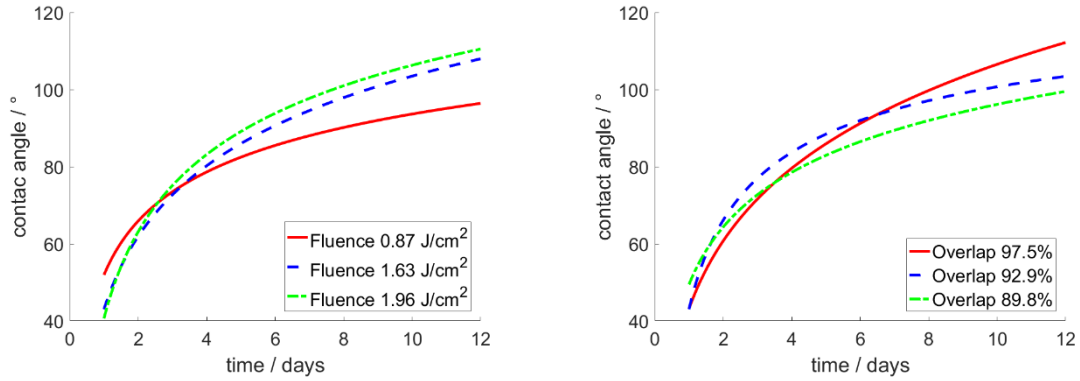

(a) (b)

Fig. 7

(a) Laser fluence and (b) pulse overlap investigation of λ=1030nm towards time

CONCLUSION

We generated laser induced periodic surface structures with low spatial frequency on CuZn30 brass using a femtosecond laser and studied the influence of laser wavelength, fluence and pulse overlap on the contact angle of a droplet destilled water and its temporal evolution during twelve days. We find that LIPSS generation using a laser wavelength of 1030 nm and 515 nm leads to an initial drop and a subsequent pronounced increase of the contact angle, whereas irradiation with 343 nm results only in an increase of the contact angle. In addition, surfaces with the highest initial drop of the contact angle exhibit after days the highest increase of the contact angle. An analysis of the LIPSS geometry leads to the assumption that a higher energy deposited into the surface region results in higher contact angles.

REFERENCES

[1] BIRNBAUM, M.: **Semiconductor Surface Damage Produced by Ruby Lasers** - Journal of Applied Physics, 1965. Vol. 36 p. 3688

[2] BONSE, J., KRÜGER, J., HÖHM, H., ET AL: **Femtosecond laser-induced periodic surface structures** - Journal of Laser Applications, 2012. Vol. 24 Issue 4 p. 042006

[3] ARDRON, M., WESTON, N., HAND, D.: **A practical technique for the generation of highly uniform LIPSS** – Applied Surface Science, 2014. Vol. 313 pp. 123-131

[4] WECK, A., CRAWFORD, T., WILKINSON, D., ET AL: **Ripple formation during deep hole drilling in copper with ultrashort laser pulses** – Applied Physics A: Materials Science and Processing, 2007. Vol. 89 Issue 4 pp. 1001-1003

[5] BOROWIEC, A., Haugen, H.: **Subwavelength ripple formation on the surfaces of compound semiconductors irradiated with femtosecond laser pulses** – Applied Physics Letters, 2003. Vol. 82, Issue 25 pp. 4462-4464

[6] HUANG, M., ZHAO, F., CHENG, Y., ET AL: **Origin of laser-induced near-subwavelength ripples: Interference between surface plasmons and incident laser** – ACS Nano, 2009. Vol. 3, Issue 12 pp. 4062-4070

[7] TEMPLE, P., SOILEAU, M.: **Polarization charge model for laser-induced ripple patterns in dielectric materials** – IEEE Journal of Quantum Electronics, 1981. Vol. 17 Issue 10 pp. 2067-2072

[8] DUFFT, D., ROSENFELD, A., DAS, S., ET AL: **Femtosecond laser-induced periodic surface structures revisited A comparative study on ZnO** – Journal of Applied Physics, 2009. Vol. 105 Issue 3

[9] WALLAT, K., DÖRR, D., LE HARZIC, R., ET AL: **Cellular reactions toward nanostructured silicon surfaces created by laser ablation** – Journal of Laser Applications, 2012. Vol. 24 Issue 4

[10] BONSE, J., KOTER, R., HARTELT, M. ET AL: **Femtosecond laser-induced periodic surface structures on steel and titanium alloy for tribological applications** – Applied Physics A: Materials Science and Processing, 2014. Vol. 117 pp. 103-110

[11] MADÉO, J., MARGIOLAKIS, A. ZHAO, Z., ET AL: **Ultrafast properties of femtosecond-laser-ablated GaAs and its application to terahertz optoelectronics** – Optics Letters, 2015. Vol. 40 Issue 14 pp. 13-19

[12] PAZOKIAN, H., SELIMIS, A., BARZIN, J., ET AL: **Tailoring the wetting properties of polymers from highly hydrophilic to superhydrophobic using UV laser pulses** – Journal of Micromechanics and Microengineering, 2012. Vol. 22 Issue 3 p. 035001

[13] FÜRSTNER, R., BARTHLOTT, W. NEINHUIS C. ET AL: **Wetting and self-cleaning properties of artificial superhydrophobic surfaces** – Langmuir, 2005. Vol. 21 Issue 3 pp. 956-961

[14] YOUNG, T.: **An Essay on the Cohesion of Fluids** – Philosophical Transactions oft he Royal Society of London, 1805. Vol. 95 Issue 0 pp. 65-87

[15] WENZEL, R. N.: **Surface roughness and contact angle** – Journal of Physical and Colloid Chemistry, 1949. Vol. 53 Issue May pp. 1466-1467

[16] CASSIE, A., BAXTER, S.: **Wettability of porous surfaces** – Transactions of the Faraday Society, 1944. Vol. 40 Issue 0 p. 546

[17] KIETZIG, A.-M., MIRVAKILI, M., KAMAL, S., ET AL: **Laser-Patterned Super- Hydrophobic Pure Metallic Substrates : Cassie to Wenzel Wetting Transitions** – Journal of Adhesion Science and Technology, 2011. Vol 25 Issue 20 pp. 2789-2809

[18] MARTÌNEZ-CALDERON, M., RODRIGUEZ, A. DIAZ, A., ET AL: **Femto-second laser manufacturing of highly hydrophobic hierarchical structures**

fabricated by combining surface microstructures and LIPSS –
Proceedings of LIM, 2015.